Acta Materialia 110 (2016) 122–130

Contents lists available at ScienceDirect

Acta Materialia

journal homepage: www.elsevier.com/locate/actamat

Full length article

Size- and phase-dependent mechanical properties of ultrathin Si films on polyimide substrates

Franziska F. Schlich, Ralph Spolenak*

Laboratory for Nanometallurgy, Department of Materials, ETH Zürich, Vladimir-Prelog-Weg 5, 8093 Zürich, Switzerland

ARTICLE INFO

Article history:
Received 1 February 2016
Received in revised form
8 March 2016
Accepted 10 March 2016
Available online 21 March 2016

Keywords:
Silicon
Metal-induced crystallization
Mechanical behavior
Thin films

ABSTRACT

Ultrathin Si films in the nanometer range are extensively used for electronic and optoelectronic devices. Their mechanical properties have a high impact on the durability of the devices during lifetime. Here, fragmentation and buckling of 8–103 nm thin amorphous and polycrystalline (poly-) Si films on polyimide substrates have been studied by *in situ* light microscopy, Raman spectroscopy and resistance measurements. Generally, a smaller film thickness and a compressive residual stress delays the fracture of the film. The fracture strength of poly-Si films is larger compared to that of amorphous Si films while the adhesion to the substrate is better for amorphous Si compared to poly-Si. The onset delamination as a function of film thickness differs for the two phases and is described by two different models. Thin-film models for fracture toughness (amorphous Si: $K_{1C} = 1.49 \pm 0.22$, poly-Si: $K_{1C} = 3.36 \pm 1.37$) are applied, discussed, and found to be consistent with literature values.

1. Introduction

Ultrathin Si films in the nanometer-range are, amongst others, implemented in solar cells [1,2], microelectromechanical systems (MEMS) [3], transistors [4–6], or interference coatings [7,8]. The functionality of the devices relies on their mechanical integrity during service life. Strain due to bending or torsion of devices on flexible substrates or thermal stress could lead to failure. Fracture toughness, which corresponds to the resistance to the propagation of cracks is a relevant factor when it comes to brittle materials such as Si. Many researchers have evaluated the fracture toughness of Si samples with different crystallographic phases and geometries: poly-Si films in the micrometer range thickness were studied extensively and a fracture toughness between 1.1 MPa $m^{0.5}$ and 4.5 MPa $m^{0.5}$ was reported [9–11]. The fracture toughness of single crystalline specimens lies around 0.8 MPa $m^{0.5}$ and 1.3 MPa $m^{0.5}$ [12,13]. Ballarini *et al.* investigated the fracture toughness of micrometer-thick amorphous Si. They determined a value of 1.0 MPa $m^{0.5}$ [14]. However, they assumed that the Young's modulus of amorphous Si is the same as that of poly-Si, which is unlikely [15,16]. Waller *et al.* determined an energy release rate of 16 J/m^2 for a 230 nm amorphous Si film (aSi:H) which corresponds to a fracture toughness of 1.2 MPa $m^{0.5}$ [17].

To our knowledge there is a lack of information on the mechanical properties of nanometer-sized Si films. It can be expected that they have much better cohesive and adhesive properties compared to micrometer thick films because of a size-effect. Moreover, it was shown that nanometer-sized Si layers on metals switch their color upon amorphization and crystallization, respectively [18]. Consequently, it is of interest to compare the mechanical properties of amorphous and crystalline Si films of various thicknesses for the application as tunable color devices. In this study, both gaps are filled by investigating the fracture behavior of 8–103 nm thick amorphous and poly-Si films on polyimide substrates. The onset strain of fragmentation and buckling, the fracture strength and the fracture toughness are obtained from uniaxial tensile tests and, these values are compared to literature values where available. The fragmentation process can be divided into three regimes [19,20]. The first regime is defect-controlled and first cracks appear as soon as the film stress exceeds the fracture strength of the largest defect. At the crossover fragmentation length L_c between the first and the second regime the stress relaxation zones start to overlap and new cracks appear mainly in the middle of a fragment where the stress is maximized. In the third regime, no additional cracks appear because the stress is compensated by delamination or substrate yielding.

* Corresponding author.
E-mail addresses: franziska.schlich@mat.ethz.ch (F.F. Schlich), ralph.spolenak@mat.ethz.ch (R. Spolenak).

http://dx.doi.org/10.1016/j.actamat.2016.03.028
1359-6454/

2. Experimental details

2.1. Sample fabrication

Thin Si films were fabricated by magnetron sputter deposition (PVD Products) with a base pressure of less than $8 \cdot 10^{-5}$ Pa. Polyimide sheets (Kapton® E from DuPont™) with a thickness of 50 μm were used as substrates. Prior to deposition the polyimide sheets were cleaned in acetone (at least 15 min) and isopropanol (at least 15 min) in a ultrasonic bath and subsequently baked in a furnace at 200 °C for at least 6 h. During sputter deposition the substrate was rotated with 30 rpm in order to achieve a homogeneous film thickness. Amorphous Si films were fabricated by alternating current sputter deposition using a power of 300 W, a pressure of 0.67 Pa and an argon flow of 50 sccm. This resulted in 8 nm, 18 nm, 25 nm, 43 nm and 96 nm thick amorphous Si films on Kapton® E. Additionally, the same thicknesses of amorphous Si films with a thin Pt capping layer were sputtered without breaking the vacuum in between for *in situ* resistance measurements. A direct current power of 100 W, a pressure of 0.67 Pa and an argon flow of 20 sccm were used for Pt.

Poly-Si was fabricated from amorphous Si by an aluminum-induced layer exchange (AILE) mechanism [21]. During this process amorphous Si diffuses into an Al film and crystallizes at the grain boundaries until a continuous poly-Si film forms at the position where previously the Al layer has been. The crystallization temperature of Si on Kapton® E must be below 400 °C because the maximum service temperature of Kapton® E is at 400 °C [22]. In this study, the film thickness of Al was always slightly thinner than that of Si (ratio approx. 5:6) in order to ensure a continuous poly-Si film [23]. First, Al was sputtered onto Kapton® E with a power of 300 W at 0.67 Pa and with an Ar flow of 10 sccm. Second, the film was exposed to air for 5 min so that a thin Al oxide layer was formed [24]. Third, amorphous Si was sputtered onto the Al layer. The rf power was adjusted to 300 W, the pressure was set to 0.40 Pa and the Ar gas flow was 50 sccm. After annealing the samples in a vacuum furnace (2 Pa) at 400 °C for 18 h the layer exchange was completed. This was confirmed by cross-sectional high resolution scanning electron microscope (SEM) images (FEI Magellan 400 FEG XHR-SEM). In a last step the Al was etched according to [25] with $16H_3PO_4$: $1HNO_3$:1 HAc: $2H_2O$ at 50 °C. Finally, the poly-Si films on polyimide had a thickness of 32 nm, 40 nm, 45 nm, 100 nm and 103 nm. Typical SEM cross sectional micrographs during the AILE mechanism are depicted exemplarily for 103 nm Si in Fig. 1 (a)-(c). The as-deposited Al and amorphous Si films on Kapton® E are shown in Fig. 1 (a). In Fig. 1 (b), the AILE mechanism was completed and the Si was crystalline after annealing. The film thickness of the as-deposited Si film was slightly larger than the Al film thickness such that some crystalline Si particles stayed in the Al film (see Fig. 1 (b)). After etching the Al film a continuous poly-Si film remains covered with some Si crystallites (see Fig. 1 (c)).

2.2. Characterization

The residual stress of the Si films was determined by two different methods: for amorphous Si the curvature of the polyimide substrates with the Si films was measured by optical microscopy and the residual stress was calculated using the Stoney equation [26]. For poly-Si films this method was not reliable because the long exposure to 400 °C results in a plastic deformation of the polyimide substrate. Consequently, the curvature did not originate only from the film but also from the substrate. Here, the stress was calculated from Raman spectra obtained from measurements with a confocal Raman system (WITec CRM200) with 441 nm excitation, a 100x objective lens with numerical aperture NA = 0.9 and a fiber-coupled grating spectrometer (2400 lines/mm). The laser intensity at the sample surface was reduced to 35.5 $\mu W/\mu m^2$ to minimize sample heating. The peak positions of the Si spectra were fitted with a MATLAB routine employing Lorentzian curves. For each film, 4 line scans with 20 spectra each were measured and the Si peak positions were averaged.

For uniaxial tensile tests, the samples were mounted into a tensile machine (Kammrath & Weiss GmbH) equipped with a 200 N load cell. Each sample was 5 mm wide and the gagelength l was 14 mm (resistance measurement) or 30 mm (optical microscopy and Raman spectroscopy measurement). The corresponding strain rates were 10^{-4} sec^{-1} and $4.7 \cdot 10^{-5}$ sec^{-1}, respectively. Crack patterns and crack distances of the films were investigated with a confocal light microscope (WITec CRM200) and simultaneous stepwise loading of the sample. The mean crack distance $<L>$ was determined with a MATLAB routine [27] based on optical micrographs. *In situ* resistance measurements of amorphous Si with a thin Pt capping layer were performed with an electrical resistance module. During uniaxial loading the current was minimized (100 mA) to prevent heating of the sample and the change of voltage was recorded. The change of the normalized electrical resistance R/R_0 with the initial resistance R_0 of the film before loading was measured for different film thicknesses. The ideal resistance of a continuous coating can be calculated from the resistivity ρ, the length L and the cross sectional area A. Assuming the volume of a coating to be constant ($A_0 \cdot L_0 = A \cdot L$) it follows that the change of the normalized resistance upon straining is $R/R_0 = (L/$

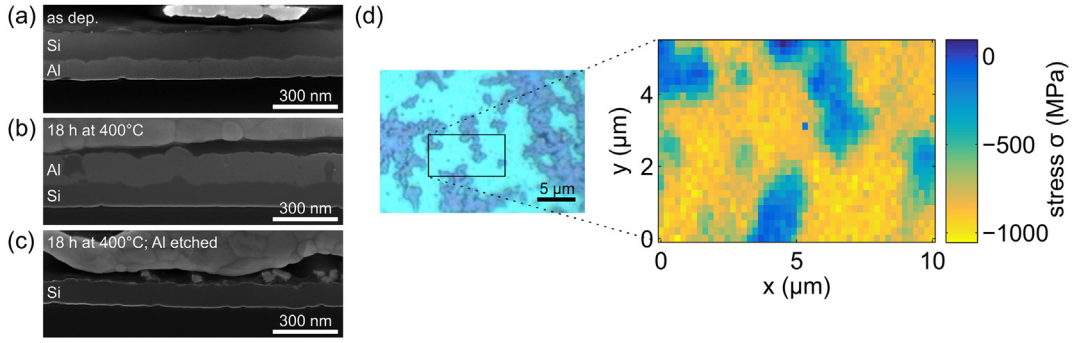

Fig. 1. Cross section SEM images of sputtered Al and Si film on Kapton® E before (a) and after annealing ((b) and (c)). On top of the films silver particles can be seen which are due to the cross section preparation process. After wet-chemical etching of the Al film (c), small Si crystallites remain on top of the continuous poly-Si layer. (d) Optical micrograph image of a 103 nm poly-Si layer with crystalline Si particles (darker features) on top. In the inset a stress map which was measured with the Raman spectroscope is shown. It indicates that the residual stress of the film is not homogeneously distributed: the residual stress is compressive where no crystalline particles can be found and it is relaxed where particles cover the poly-Si layer.